THE GLOBAL CIRCUIT INTENSITY

Its Measurement and Variation over the Last 50 Years

BY RALPH MARKSON

Ionospheric potential measurements can quantify the intensity and variation of Earth's atmospheric electric global circuit and contribute to understanding global change.

A fundamental problem in atmospheric electric research has been the measurement of the intensity and variation of Earth's electric field, which is proportional to ionospheric potential (Vi). This paper describes the measurement of Vi and the factors affecting it, compares the annual variation of global lightning activity, and discusses the natural (temperature and cosmic radiation) and manmade (nuclear debris) effects on the global circuit as inferred from Vi variation.

Furthermore, the analysis reported here shows that aircraft and balloon measurements of Vi so far support the global circuit hypothesis. This hypothesis (that all thunderstorm activity maintains Earth's electric field) has been questioned in the past because of the difficulty of making reliable globally representative measurements (Dolezalek 1971; Bering et al. 1998). Now, at a time when interest in the atmospheric electrical global circuit has increased because of global change concerns, such measurements exist. They demonstrate the validity of the hypothesis, with an exception first suggested by Wilson (1920), that electrified shower clouds also contribute significantly to the current flow in the circuit.

Since the convective clouds that maintain the global circuit and associated fair-weather electric field are modulated by heating of Earth's surface, temperature variation can affect global circuit intensity. This raises the possibility that monitoring the global circuit, which has the advantage of being possible with single measurements, could be a convenient tool for monitoring global temperature change. Already, investigations have shown positive correlation between one-hour-resolution continental-scale temperature over land and Vi, a measure of Earth's fair-weather electric field intensity. However, a negative feedback exists over continents: higher-than-normal morning temperature causes enhanced convective activity early in the day causing more cloudiness, which reduces solar heating in the afternoon. This would stabilize or reduce the rate of warming on the diurnal time scale of surface air over land. Enhanced convection also increases nighttime cloudiness and water vapor in the upper troposphere, decreasing nighttime radiational cooling. Since most of the reported global warming signal comes from higher nighttime temperatures, this suggests the importance of thunderstorms and other convective clouds in global warming—they are the source of water vapor, the most important greenhouse gas.

AFFILIATIONS: MARKSON—Airborne Research Associates, Weston, Massachusetts
CORRESPONDING AUTHOR: Ralph Markson, Airborne Research Associates, 46 Kendal Common Road, Weston, MA 02493
E-mail: rmarkson@comcast.net

The abstract for this article can be found in this issue, following the table of contents.
DOI:10.1175/BAMS-88-2-223

In final form 31 August 2006
©2007 American Meteorological Society

While my analysis of current and historical balloon and aircraft measurements of Vi shows little variation over the last 50 years from a mean value of about 240 kV, the period of atmospheric nuclear testing in the late 1950s and early 1960s is a clear exception. The positive correlation between Strontium-90 (Sr-90) in the stratosphere and Vi is consistent with the hypothesis that the variation of ionization in the lower stratosphere and upper troposphere due to solar modulation of cosmic radiation, the primary source of atmospheric ionization, changes global circuit intensity and does so in the generator part of the circuit but not in the fair-weather return-path regions (Markson 1978).

STRUCTURE OF THE GLOBAL CIRCUIT. The spherical capacitor structure of the Earth's geoelectric field constitutes a unique geophysical system in which the intensity and variation of the global circuit can be determined by monitoring Vi, the electrical potential of the highly conductive lower ionosphere relative to the Earth's surface. Thus, a single reliable measurement of Vi at mid- or low latitude provides a measure of Earth's fair-weather electric field intensity and the current in the global circuit worldwide, except in polar cap regions where upper-atmosphere generators are present.

The global circuit concept of the Earth and ionosphere resembling the conductive shells of a spherical capacitor, with the atmosphere as a leaky dielectric between them, was proposed by C. T. R. Wilson (1920). He suggested that thunderstorms and electrified clouds in stormy weather regions were generators maintaining the current. This model followed postulation of an ionized layer in the upper atmosphere to explain long-range radio transmission (*Encyclopedia Britannica,* tenth ed., s.v. "telegraphy"). Even earlier, Lord Kelvin noted that the upper atmosphere contained a conducting layer and described the spherical capacitor model for Earth's atmospheric electric field with negative charge on the Earth's surface and positive charge mostly in the lower atmosphere. However, he did not explain the maintenance of the electric field (Lord Kelvin 1860).

Thunderclouds and some shower clouds cause conduction currents to flow upward over them and the current flows all over the world in the highly conductive region near the bottom of the ionosphere to return to the Earth in the fair-weather (nonthunderstorm) regions as the air–Earth conduction current (Chalmers 1967, p. 216). The circuit is completed beneath thunderstorms by corona from points on the ground, conduction, convection, and rain currents, plus lightning, which on average transport negative charge from cloud base to the ground. Over much larger areas than those occupied by thunderstorms there are weaker conduction currents that apparently integrate to a larger current than those in thunderstorm areas (Williams and Heckman 1993). These currents maintain the fair-weather electric field, averaging about 130 V m^{-1} near the ground (Chalmers 1967, p. 450; Israël 1973, p. 338). This circulation of charge is called the global circuit current. If the global generator stopped abruptly, Earth's fair-weather electric field would decay to 5% of its original value in an hour because of atmospheric conductivity. This does not happen because somewhere there always are active thunderstorms and electrified shower clouds maintaining the global circuit current.

The spherical capacitor model has an outer shell at the lower edge of the ionosphere at a height of about 60–70 km where free electrons begin to dominate electrical conductivity, causing a sharp increase in conductivity with height (electrical relaxation time on the order of 100 μs.) Because of high conductivity there is very little space charge in the upper atmosphere; most occurs in the lower atmosphere where conductivity is much smaller. The inner shell, Earth's surface, is also highly conductive (relaxation time about 0.03 μs). The atmosphere is a weakly conductive medium between these spherical shells; its conductivity, maintained mostly by galactic cosmic radiation, is thus at a minimum near the ground (relaxation time about 1000 s). Aerosols, concentrated in the planetary boundary layer, lower the conductivity in this region while radon and radioactive emanations from the ground increase conductivity in the lowest tens to a few 100 m of the atmosphere over most land areas. The outer shell of the capacitor, being highly conductive, is effectively an equipotential surface over most of the world. However, upper-atmosphere electromagnetic generators in the polar-cap region (about 23° from the magnetic poles) vary with solar activity and can superimpose a few tens of kV on Vi locally (Richmond 1986; Roble and Tzur 1986).

Ionospheric potential variation cannot be measured reliably with electric field instruments at the Earth's surface over land, sea, or ice due to local anthropogenic and natural factors because there are many processes influencing the fair-weather electric field and air–Earth conduction current, including 1) manmade and natural aerosols that change conductivity; 2) the breaking of sea bubbles (Blanchard 1963) and the electrode effect (Chalmers 1967, p. 42), both creating positive space charge concentrated within a few tens of meters of the ocean surface, which through turbulence cause

10%–50% variations in electric field intensity over periods of seconds to minutes (Markson 1975); 3) the electrode effect also occurs over ice fields (Kraan 1971, p. 47) and land regions that do not contain ionization sources (uranium and radon); 4) electrified ice crystals in the air in regions of snow and ice (Chalmers 1967, p. 75); 5) space charge and aerosols emitted by engines, fires, and industry; 6) changes in the air–Earth current and thus the electric field caused by the lower conductivity (higher resistance) of cloud layers; 7) electrification from some clouds; 8) the modulation of electric fields by high objects, such as trees and buildings, in the vicinity of the sensor (Chalmers 1967, p. 136); and 9) conductivity variations caused by changes in the mobility of ions affected by relative humidity variations [particularly near the deliquescence point at about 80% relative humidity (RH); Pruppacher and Klett 1978; Markson et al. 1999]. Air motion causes spatial and temporal variations of these elements. Because of these factors, electric field sensors at the Earth's surface cannot routinely obtain electric field data representing global circuit variation. A correlation analysis of electric field data from 179 land station pairs at 20 global locations found only one pair had a statistically significant correlation from the closest pair of stations 60 miles apart (Bhartendu 1971). Another limitation of ground-based measurements is that they cannot measure Vi magnitude; this requires a vertical electric field sounding through the atmosphere.

One of the best ground-based studies of the global circuit variation used measurements made on Hawaii's Mauna Loa Mountain (Cobb 1968). This mountaintop, at 3.4 km, is generally above the inversion and, in the central Pacific, is distant from sources of pollution. During fair-weather periods the air–Earth current variation often resembled the Carnegie curve, the average diurnal variation of electric field intensity over the ocean (Chalmers 1967, p. 164); however, the mountain is covered with an electrode layer of positive space charge enhancing the electric field causing atmospheric electric variations as a function of wind and turbulence moving space charge. In a balloon sounding at Mauna Loa Observatory, an electrode layer 100 m thick was observed causing a doubling of electric field intensity in the lowest 100 m (Markson and Kendra 1992). Another problem with this site is that "the observatory is commonly engulfed in cloud during the afternoon" (Cobb 1968).

VERIFICATION OF THE GLOBAL CIRCUIT HYPOTHESIS. According to the global circuit/spherical capacitor model, Earth's electric field intensity should vary on the order of one second worldwide. Aircraft and balloon electric field measurements provide methods to measure the global circuit magnitude and variability. Three approaches to these measurements have been pursued: 1) constant altitude time series measurements of electric field or air–Earth current over a diurnal cycle at remote fair-weather locations with few or no clouds above or below the measuring platform should be well correlated with each other and with the Carnegie curve as both are proportional to Vi (Markson 1976, 1985), if a well-defined Carnegie curve variation (defined by Whipple and Scrase 1936) is not seen every day, the measurement is not globally representative since deep convection maximizes over the continents every afternoon and the continents do not move, 2) a time series of Vi soundings over a full day or substantial portion of a day should be well correlated with the Carnegie curve, and 3) simultaneous measurements of Vi at remote locations should have the same magnitude (Mühleisen 1971; Markson 1985; Markson et al. 1999).

DIURNAL VARIATION. A pronounced characteristic of the Earth's electric field is its diurnal variation as found originally in analysis of electric field measurements by the magnetic survey ships, *Maud* and *Carnegie,* on global cruises during 1915–29 (Ault and Mauchly 1926; Torreson et al. 1946). The investigators hoped that measurements in clean ocean air, away from local environmental noise sources, would provide globally representative data not available from land stations. When the ship's lowest noise measurements (a small fraction of the data) were averaged over many days according to the UTC when obtained, the classic Carnegie curve emerged. This quasi-sinusoidal variation, with a peak-to-peak excursion of +19% to −14% from the mean, was obtained from a statistical average of the best 130 days of data taken from several years of measurements (Kasemir 1972, p. 71); but rarely seen in a single day's data. Subsequently, it was found that the Carnegie curve average diurnal variation closely resembled the average UTC variation of global thunderstorm activity (Whipple and Scrase 1936); this correlation (Fig. 1) constituted the basic evidence for the global circuit hypothesis for many decades. The maximum occurs in the 1800–2000 UTC interval due to superposition of peak afternoon thunderstorm activity over Africa and the Americas. The minimum occurs in the 0100–0600 UTC interval when the sun is over the Pacific where there is little land to heat and relatively few thunderstorms. Because of local noise, positive correlations of the vertical electric field on minute-by-minute or hour-by-hour time series had

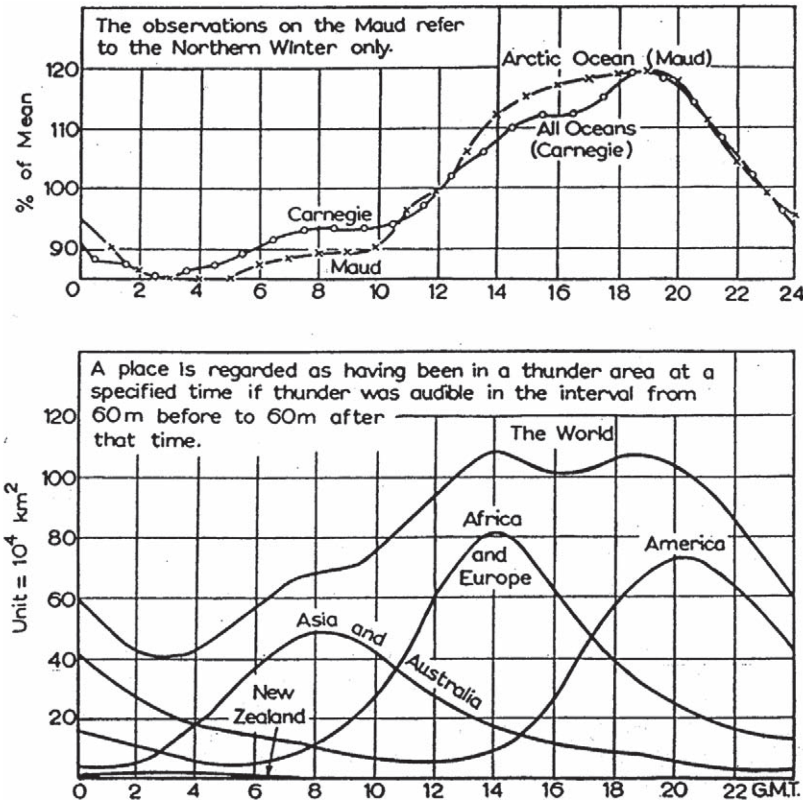

Fig. 1. Diurnal variation of electric field in unperturbed conditions over (top) the oceans and (bottom) thunder areas. [From: Whipple and Scrase (1936), reproduced from Chalmers (1967)].

never been reported between remote locations in different parts of the world until this was accomplished in 1972 using simultaneous measurements by aircraft in oceanic regions in the Bahamas and Gulf of Alaska 7000 km apart (Markson 1976). In this experiment, continuous measurements of vertical electric field intensity and 15-minute-resolution air–Earth current were made through a diurnal period. These time series were both well correlated with each other and the Carnegie curve, providing the first fine time resolution measurements of the global circuit supporting the global circuit hypothesis.

MEASURING THE VARIATION OF GLOBAL CIRCUIT INTENSITY AND VI SOUNDINGS.

The most reliable measurement of Earth's geoelectric potential that avoids contamination by the various local effects noted above is to make electric field profile soundings and integrate the results from the ground up to the ionosphere (Clark 1958; Fischer 1962; Markson 1976). Soundings through a vertical column of the atmosphere minimize effects of electrode-layer space charge and other noise sources near Earth's surface; this region occupies only a small fraction of the total integrated path. The most favorable locations for soundings are clean-air ocean regions with no clouds, or only scattered clouds that can be avoided (Clark 1958). Because the electric field decreases quasi exponentially with height, from about 130 V m^{-1} near the surface to about 15 V m^{-1} at 5 km and 5 V m^{-1} at 10 km, it is unnecessary to make very high soundings to determine Vi. The potential difference between ground level and sounding top is measured directly, the remainder can be extrapolated accurately as the variation of electric field with altitude has a known exponential decrease with altitude once above the lower atmospheric region of varying conductivity. Potential difference between sounding top and ionosphere can be computed from the scale height of the sounding at apogee times electric field intensity at apogee (Markson 1976). Adding the computed increment to the integrated potential of the sounding gives Vi. Since most of the Earth-to-ionosphere potential difference lies in the low conductivity exchange layer below the inversion (generally not over 3 km), soundings extending above about 4 km often can be used for Vi estimates, although higher soundings are preferred. The profile shows that an acceptable height was reached when the inversion level is clearly delineated (there is a characteristic sharp increase in conductivity and corresponding decrease in electric field); above the inversion there is an exponential decrease in electric field and increase in conductivity with height. The sounding must extend sufficiently above the inversion to obtain a measure of the scale height needed to compute the extrapolated potential. By 5 km, 80% of Vi has been crossed (Markson 1976), thus a 5% error in the extrapolated remaining 20% of Vi would lead to an overall error of only 1%.

To understand the measurement of Vi, it is instructive to see what reliable electric field soundings look like. Figure 2 shows almost simultaneous electric field (E) soundings by two aircraft over the ocean 100 km apart (Markson 1985). The variation of atmospheric potential with height (V), calculated by integrating the electric field, is shown. The close parallel of variations in the profiles is caused by horizontally stratified air layers. The top of the exchange layer is at 1.4 km. Here the electric field drops sharply because of its inverse relationship to conductivity. At any time and location over time scales longer than about 1 second and away from local electrical generators, the electric field times conductivity (the air–Earth conduction current density) is constant with altitude through the atmosphere. Both electric field and conductivity are measured during the aircraft soundings and the computed air–Earth current density being constant with altitude confirms that both instruments are working correctly. Above the inversion, conductivity increases rapidly as the lower mobility hydrated aerosol are confined to the marine boundary layer; an exponential decrease in *E* occurs because of the increase in cosmic ray ionization with altitude. This figure illustrates how, in favorable regions, it is not necessary to make very high soundings to obtain reliable estimates of Vi; cross calibration between independently calibrated aircraft indicates the reliability of the measuring technique.

Figure 3a, a balloon electric field profile in clean air in the middle of the Pacific Ocean (Hawaii), illustrates that in this case above 1 km, electric field intensity is controlled by cosmic radiation. This sounding shows an unusual electrode space charge layer near the ground, an inversion at 1 km, and the characteristic exponential decrease in *E* above. It also indicates a thin layer of enhanced *E* at about 3 km probably caused by lower conductivity in a thin cloud layer. Figure 3b, a log-linear plot of the sounding, shows a straight line indicating that the curve is exponential. Integration of this sounding gives a potential at the 10.9-km sounding apogee of 218 kV; the remainder from the top of the sounding to the ionosphere is 14 kV giving a total Vi of 232 kV.

Aircraft soundings are preferable to balloon soundings for several reasons. They can provide complete up and down profiles one half-hour apart on the same flight in the same local air mass. Balloon soundings provide only a complete up sounding since, in the hour required for the balloon to complete the up sounding, it typically drifts 10–50 km downwind. The up sounding ends when the balloon breaks: this is set for about 10 km since there is no need to go higher as this height is through 90% of Vi. Then a down-parachute sounding is made as the radiosonde drifts further downwind. Usually data can not be obtained from the lowest 1 or 2 km of down soundings because the telemetry is line of sight. This is a critical limitation because about one-quarter to one-half of Vi occurs below that height, preventing comparison of up and down Vi measurements useful for verifying reliability. Also, the air mass 10–50 km away may have clouds or other factors such as low-mobility aerosols that would change the columnar resistance (Chalmers 1967, p. 210), introducing error into the measurement.

The estimated accuracy for the Mühleisen and Fischer balloon soundings, ±8%, was an average of the estimated errors from all unspecified sources as listed by Fischer (1962). The 1995 balloon soundings (Markson et al. 1999) had an estimated accuracy on the order of ±6%. Subsequent balloon soundings used improved instrumentation, so the same or better accuracy is assumed.

Aircraft measurements of Vi have an important advantage in using the same instrument for all soundings eliminating differences between calibra-

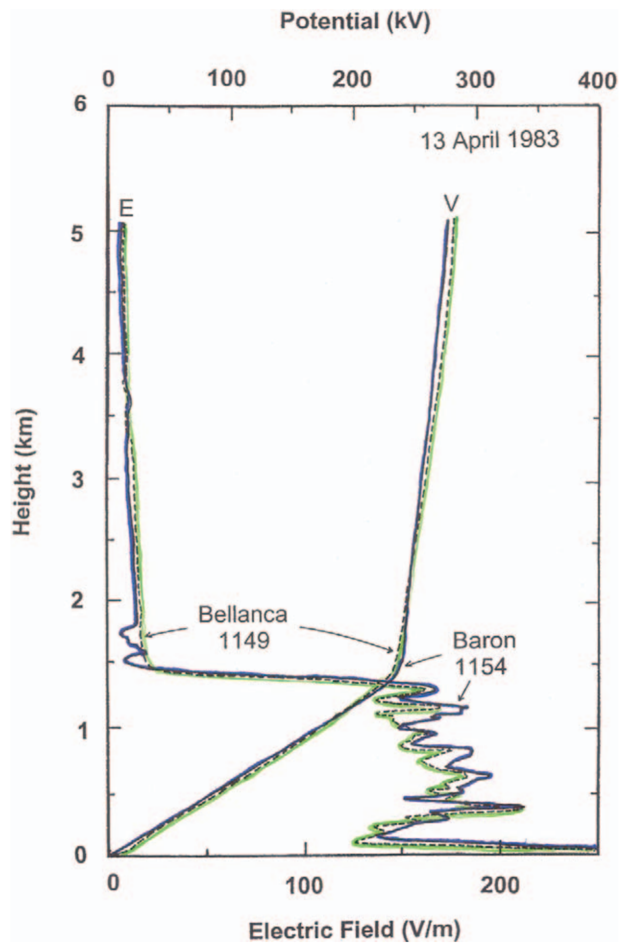

Fig. 2. Two almost simultaneous electric field soundings (*E*) from aircraft 100 km apart over the ocean off of Virginia illustrating the electrode layer close to the ocean, the exchange layer up to 1.4 km, and the low-noise exponential region above the exchange layer. The integrated potential variation with height (*V*) is shown. The close match of the two profiles indicates the reliability of the measuring procedure.

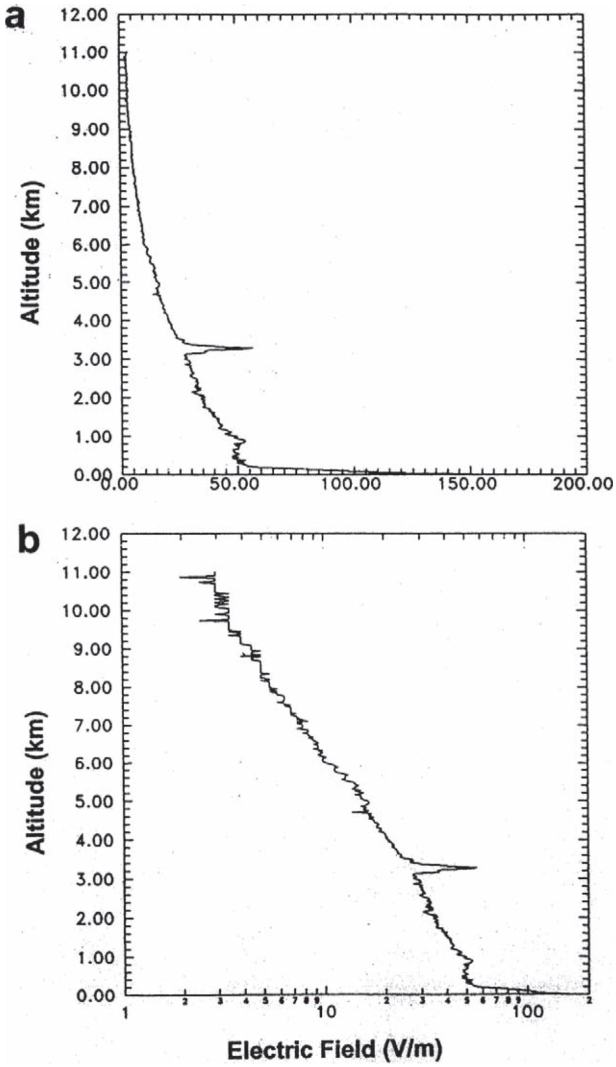

FIG. 3. Balloon electric field sounding in clean air at Hilo, Hawaii. (a) The electrode layer shown near the ground (typical for oceans) exists here because there is no radiation or radioactive gases in the volcanic soil that would increase ionization in the lower atmosphere. The top of the exchange layer is at 1 km and a thin cloud or aerosol layer is at 3 km. (b) The sounding being straight on a log-linear plot illustrates the decrease with altitude is exponential and controlled by cosmic radiation. If the variation above the exchange layer is not exponential the data would be questionable, indicating the presence of local atmospheric or instrumentation factors influencing the sounding. (The horizontal variations near the top of the sounding are due to digitization.)

tion of different sensors, thus providing reliability in analysis of relative changes in Vi over extended periods—years to decades. All electric field data from Clark were obtained using a single system with an estimated accuracy of ±10% (Clark 1958). The data from Markson in 1971–72 were made with a single system from an aircraft. During the period 1980–82 two similarly instrumented aircraft were operated and cross calibrated (Fig. 2). One of these aircraft has been used since 1983 with estimated accuracy of ±5% and estimated precision of ±3%. For Vi soundings the aircraft is kept in a 10° bank to make a spiral sounding of a few miles diameter to stay in the same columnar resistance volume in a cloud-free region; this reduces the vertical field component by 1.5%, which is allowed for in data analysis.

NATURAL SOURCES OF SPACE CHARGE NEAR THE EARTH'S SURFACE: THE ELECTRODE LAYER. An unusual feature in Fig. 3 is the large increase in electric field close to the ground due to a layer of positive space charge in the lowest 200 m. While a layer of positive space charge near the water is always observed over the ocean, this is the first reported sounding showing such an effect over land. (Space charge density is the difference between the number of positive and negative ions in a volume.) This space charge layer is caused by the accumulation of positive ions drifting downward in the fair-weather electric field, which is not counterbalanced by negative ions drifting upward. An electrode layer does not form over most land areas because much of the Earth's land surface contains uranium and radon causing ionization of air molecules of both polarities close to the ground. Thus, in the fair-weather electric field just above the ground in most areas, there are negative ions that drift upward into the volume immediately above the ground at about the same rate as the positive ions drifting downward and there is no accumulation of positive space charge. However, near the ocean surface, ionization of air molecules from sources in the ground is not present so there are no negative ions and the electrode layer forms. The electrode-layer space charge is carried upward by eddy diffusion in decreasing concentration to a height of about 100 m (Markson 1975; Fig. 4). Since Hawaii is volcanic, there is no uranium or radon in the ground and an electrode layer forms.

Space charge over bodies of water would have created enhanced and variable electric fields affecting the Carnegie data, often assumed to be a standard for past electric field measurements. The Carnegie would have been sailing in the layer of positive space charge always present over the ocean. Positive space charge from jet drops caused by the breaking of sea bubbles on days with whitecaps, the Blanchard effect (Blanchard 1963), also contributes to positive space charge near the ocean surface. Thus, in the lowest 100 m above the sea there is always a positive space charge layer causing the field intensity to increase by about 10%–50% and the positive space charge density to increase by a factor of 10 or more (Markson 1975). The space charge is moved by wind and turbulence causing electric field variations. Thus, the Carnegie electric field data would have been influenced by local meteorological conditions and sea state, which would have varied with season and location. If the Carnegie was sailing in the Northern Hemisphere winter in a region of low winds, where the electrode effect is strongest and the turbulent mixing weakest, its data would have indicated that the global electric field intensity maximized in this season, which is the opposite of the findings of the subsequent long-term Vi measurements.

ARCTIC AND ANTARCTIC MEASUREMENTS. Investigators have attempted to measure the global circuit variation in the Arctic and Antarctic because of the lack of pollution, but electric fields in such locations are affected by several environmental conditions. Since there is no ionizing radiation from the ground there is an accumulation of positive space charge in an electrode layer above the ice surface. In addition, there are electric fields caused by electrified ice crystals in the air. Measurements of electric field variation with height in Antarctica were made during the Belgian–Netherlands Antarctic Expedition (February 1966–February 1967; Kraan 1971). They found a doubling of electric field intensity from a height of 5 m to the surface with the effect larger in low-wind conditions when there is less upward eddy diffusion of the space charge (Kraan 1971, p. 44). Their balloon electric field profiles generally display significant variations from the expected exponential decrease with altitude indicating local sources of electric charge and particles aloft making these data unreliable for Vi measurements—such variations are not seen in fair-weather soundings made in other parts of the world. Often the lower part of the sounding in the 1–3 km height range shows an increase in electric field with altitude. These effects can be caused by triboelectric-charged ice particles created and carried aloft by the wind. The normalized (Carnegie curve diurnal variation removed) Vi value of these measurements is 222 kV. These data have not been included in the Vi summary because the profiles indicate they have been influenced by local factors and in 11 of the 17 soundings the lowest 1/2 to 1 km of the sounding is missing.

In addition there is persistent fallout of ice crystals from the clear sky at Vostok (magnetic South Pole), which occurs on average 247 days per year. These deposit on the ice surface "a thin loose layer easily moving with weak winds" (Pomelov 2003).

A rapid increase in electric field intensity near the surface of the ice field initiated at varying wind velocities has been reported at Vostok where a diurnal variation in wind velocity commonly occurs (Burns et al. 2005). A diurnal wind speed variation is observed nine months a year (data available online from Station Vostok, surface wind and air pressure field, at www.aari.ru/south/stations/vostok/vostok_en.html). Such a daily variation in wind velocity in a location with space charge and loose ice crystals will produce a diurnal variation of electric field intensity, but it will not be in phase with the Carnegie curve diurnal variation.

An additional problem in trying to study the global circuit in the polar-cap region is that ionospheric electric fields map downward to the Earth's surface (Richmond 1986; Roble and Tzur 1986; Burns et al. 2005) and are superimposed on the fields of the global convective cloud generator. Considerable progress has been made in removing global electric fields from Antarctic data. Earlier measurements (Bering et al. 1998) showed a maximum in the diurnal variation in the 0800–1600 UTC interval for spring/summer and in the 1200–1600 UTC range for autumn/winter, which is different than the maximum in the 1800–2000 UTC period for the Carnegie curve at all times of the year (Israël 1973, p. 353). More recent analysis (Burns et al. 2005) shows the Carnegie curve when two-month daily averages are compiled. This improvement is due to careful selection of fair-weather days (39% of the days in a 5-yr period) and correction for the polar-cap ionospheric generator. This report shows no single-day records. These results suggest that the Antarctic electric field measurements are similar to those made on the Carnegie in which the classic diurnal variation is not routinely seen on individual days but it only emerges when many days are averaged.

TESTING RELIABILITY OF VI MEASUREMENTS. *Comparison of Vi with the Carnegie curve.* Many years of experiments using a variety of techniques have demonstrated that the most robust method for measuring the global geoelectric potential magnitude and variation is a series of Vi soundings over a period of time. It is best if the period extends for 24 hours, or at least a significant portion of a day, for comparison with the Carnegie curve; if the correlation is good, the implication is that the measurements are globally representative. Good correlation between ground-level electric field data and the Carnegie curve is rarely seen in a single day's records, even on a small pollution-free island in the mid-Pacific (Markson and Kendra 1992). In the Arctic and Antarctic "usually it requires 7 to 10 day averaging for the oceanic pattern (i.e., Carnegie curve) to emerge" (Kasemir 1972, p. 75). However, the correlation of Vi time series with the Carnegie curve in a single-day time series has occurred each of the four occasions this experiment has been conducted utilizing aircraft measurements over the ocean or balloon soundings in clean, dry air over land:

1) A series of six simultaneous aircraft Vi soundings with an aircraft at Schefferville, Quebec, Canada, and another near Boston, Massachusetts, over a half-day period in 1983 showed high correlations for each aircraft and the Carnegie curve: $R = 0.97$, ($p<0.01$) for both aircraft (Markson 1985).
2) A series of 29 Vi soundings made by an aircraft 100 km off the Virginia coast in 1983: $R = 0.53$ ($p<0.01$; Markson 1985).
3) A series of 22 Vi aircraft soundings over the ocean 20 km east of Portsmouth, New Hampshire, over a half-day period in 1984: $R = 0.97$ ($p<0.0001$; Markson 1986).
4) The last such time series was at Darwin, Australia, in 1995 in a low aerosol semi-arid environment (Markson et al. 1999). Soundings were made every 3 hours on two different days. On the first day the nine Vi measurements averaged about 3% different than the Carnegie curve: $R = 0.67$ ($p<0.01$). On the second day, 10 measurements averaged 7% different than the Carnegie curve: $R = 0.88$ ($p<0.01$).

It is not expected that the correlation will be perfect; aside from measurement error, the Carnegie curve is an average of many days and each individual day will not be identical to the long-term average.

Simultaneous measurement of Vi at remote locations. Another method to verify the global circuit hypothesis and measurement reliability is comparison of simultaneous Vi soundings at remote locations. If the lower ionosphere is an equipotential, electric field profiles at any location away from the polar-cap regions should integrate to the same potential. This has been done four times: 1) between the equatorial Atlantic and southern Germany 8000 km away (Mühleisen 1971), 2) between Schefferville, and Boston 1300 km away (Markson 1985), 3) between 100 km off the coast of Wallops Island, Virginia, and the coastline (Markson 1985), and 4) between Darwin, and Weston, Massachusetts, 17,000 km away (Markson et al. 1999).

The mean difference between 15 simultaneous balloon soundings between the equatorial Atlantic and Germany was 2% (Mühleisen 1971). The difference between the means of six simultaneous aircraft soundings at Schefferville and Boston was 4.5%. Schefferville is in the polar-cap region and when the potential due to the ionospheric generator was removed the difference in Vi between the two locations was 1% (Markson 1985).

The difference between the means of 29 simultaneous aircraft soundings 100 km off the Virginia coast compared to measurements at the coastline was 4% (Markson 1985). The Darwin-to-Weston comparison of Vi magnitude from balloon soundings was unreliable because of inflated Vi values at Weston due to high humidity near the ground, particularly at night (Markson et al. 1999).

SECULAR VARIATION OF VI. Figure 4 summarizes the measurements of the three groups conducting reliable Vi measuring programs during

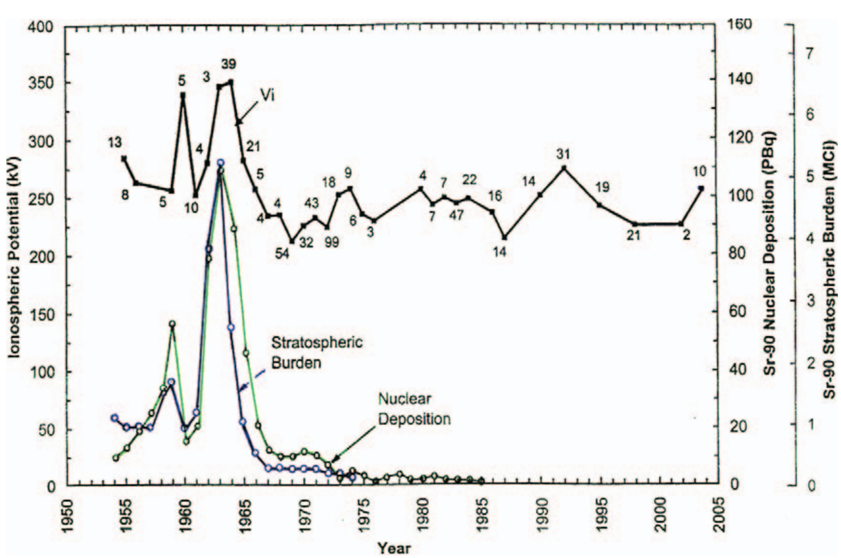

Fig. 4. Variation of ionospheric potential from 1955 to 2004. The number of soundings used for each year are given. Also shown is nuclear deposition indicating radioactive Sr-90 fallout on the ground while the stratospheric burden is a measure of Sr-90 in the stratosphere (see text for radioactivity sources).

the last 50 years. Table 1 lists details of these measurements.

The global circuit diurnal variation will affect Vi magnitude because the soundings were made at different UTC times. Assuming the Carnegie curve represents the average diurnal variation, measurements made near 1900 UTC will on average be about 33% greater than those made near 0400 UTC. To remove this effect as much as possible, the Carnegie curve percent deviation from its mean value was added or

Table 1. Details of ionospheric potential soundings.

Year	Vi	N	Observer	Aircraft/Balloon	Location
1955.9	284	13	Clark	A	Atlantic, Pacific, Greenland
1956.3	263	8	Clark	A	Atlantic, Pacific
1959.7	256	5	Mühleisen and Fischer	B	South Germany
1960.5	338	5	Mühleisen and Fischer	B	South Germany
1961.3	252	10	Mühleisen and Fischer	B	South Germany
1962.5	280	4	Mühleisen and Fischer	B	South Germany
1963.5	345	3	Mühleisen and Fischer	B	South Germany
1964.5	349	39	Mühleisen and Fischer	B	South Germany
1965.5	282	21	Mühleisen and Fischer	B	South Germany
1966.4	257	5	Mühleisen and Fischer	B	South Germany
1967.5	234	4	Mühleisen and Fischer	B	South Germany
1968.3	235	4	Mühleisen and Fischer	B	South Germany
1969.5	212	54	Mühleisen and Fischer	B	South Germany, Atlantic
1970.6	225	32	Mühleisen and Fischer	B	South Germany
1971.4	245	22	Mühleisen and Fischer	B	South Germany
1971.9	220	21	Markson	A	Bahamas
1972.1	217	78	Markson	A	Bahamas
1972.5	255	21	Mühleisen and Fischer	B	South Germany
1973.7	252	18	Mühleisen and Fischer	B	South Germany
1974.7	257	9	Mühleisen and Fischer	B	South Germany
1975.5	235	6	Mühleisen and Fischer	B	South Germany
1976.3	229	3	Mühleisen and Fischer	B	South Germany
1980.9	256	4	Markson	A	Bahamas
1981.7	243	7	Markson	A	U.S. mid-Atlantic offshore
1982.5	249	4	Markson	A	U.S. mid-Atlantic offshore
1982.8	282	3	Markson	A	U.S. mid-Atlantic offshore
1983.2	316	3	Markson	A	Boston region
1983.3	251	29	Markson	A	U.S. mid-Atlantic offshore
1983.4	206	6	Markson	A	Schefferville (Quebec)
1983.4	209	5	Markson	A	New Hampshire offshore
1983.7	240	4	Markson	A	Spitzbergen ocean
1984.8	248	22	Markson	A	New Hampshire offshore
1986.4	236	16	Markson	A	Hobbs (New Mexico)
1987.2	213	14	Markson	A	Bahamas
1990.7	248	2	Markson	B	Hawaii
1990.9	252	12	Markson	B	Christmas Island
1992.7	275	31	Markson	B	Boston area over land
1995.4	242	19	Markson	B	Darwin (Australia)
1998.2	225	21	Markson	B	Orlando (Florida)
2002.4	225	2	Markson	A	Bahamas
2004.5	250	4	Markson	A	New Hampshire offshore
2004.6	258	6	Markson	A	Bahamas

Clark's Vi data are from his Ph.D. thesis 1956. The Vi data from Mühleisen and Fischer are from the report "The Ionospheric Potential and the Solar Magnetic Sector Boundary Crossings," H. J. Fischer and R. Mühleisen, Feb. 1980, *Astonomisches Inst. der Univ. Tübingen, Aussenstelle Weissenau,* personal communication, and from Fischer 1962. Markson's data are from Markson and Muir 1980, Markson et al. 1999, and from unpublished personal records.

subtracted from the measured values of Vi depending on the time of the measurement, for example, if a Vi sounding was conducted at 1900 UTC, 19% was subtracted. This normalizes the measurements for comparison. These normalized Vi values, averaged for the year they were obtained or over specific field periods intervals are used in Fig. 4. The mean of all yearly averages is 254 kV. The mean since 1966 following the anomalous period of nuclear testing (to be discussed) is 240 kV.

Recent reports based on ground-level electric field data in England (Harrison 2002) and Hungary (Märcz and Harrison 2003) conclude that the global circuit intensity has decreased by about half or more during the twentieth century. This conclusion is questionable since these measurements would have been influenced by the large air pollution decreases in England during this period (Williams 2003). Air quality particularly improved in the United Kingdom following the deadly pollution period in 1952; a factor-of-5 decrease in black carbon emissions in the United Kingdom between 1950 and 1999 has been reported (Novakov et al. 2003).

The cleaner air would have increased conductivity and decreased electric field intensity. The Hungarian data show a 44% decrease in electric field in 39 years, that is, 113% per century. These data were obtained near a group of growing trees close to the measuring site (Märcz and Harrison 2003). The reported values, starting at 66 V m^{-1} in 1962 and ending at 37 V m^{-1} in 2001 are 1/2 to 1/3 of the typical fair-weather electric field intensity of about 130 V m^{-1} (Chalmers 1967, p. 202; Israël 1973, p. 338). Recent measurements at different distances from the straight edge of a forest and modeling show that the tree growth can account for the decrease in electric field intensity in Hungary (Williams et al. 2005). Some of the vertical electric field lines would have bent and connected to the treetops reducing electric field intensity at the nearby electric field sensor. These reports illustrate problems associated with trying to use ground-level electric field measurements to monitor the global circuit.

EFFECT OF ATMOSPHERIC NUCLEAR TESTING. Figure 4 depicts the annual variations of nuclear fallout from Sr-90 on the ground and in the stratosphere. Sr-90 is a radioactive element that ionizes air molecules. The anomalous peaks in Vi and nuclear radiation occur at about the same time. There is high correlation between Vi and nuclear radiation with Vi lagged one year. The time between atmospheric nuclear explosions and accumulation of nuclear material in the atmosphere involves complex meteorological and radioactive decay processes varying from days to years: the average is on the order of 1 yr (Glasstone and Dolan 1977, 442–450; UNSCEAR 2002, 159–167). The annual variation of Vi displays high values in 1960, 1963, and 1964. After World War II, atmospheric nuclear testing had been going on from the early 1950s until the end of 1962, and their frequency rose sharply in the years just before the test ban treaty was due to go into effect in 1963.

Two analyses were conducted. The first used nuclear deposition of Sr-90 on the ground where data for comparison with Vi are available for the period 1954 through 1985 (UNSCEAR 2002, 159–167). Figure 5 shows the correlation between nuclear deposition and Vi lagged 1 yr, about the average time it takes for fallout to reach the ground (UNSCEAR 2002, p. 162): $R = 0.79$ ($p<0.001$), with no lag $R = 0.70$ and with a lag of 2 yr $R = 0.35$. The correlation maximizing with a lag of 1 yr is in agreement with the 1-yr average atmospheric residence time for nuclear fallout (UNSCEAR 2002, p. 162).

Atmospheric nuclear testing distributes radioactive debris into the troposphere and stratosphere. Smaller ground tests do not penetrate the tropopause and reach the stratosphere, their debris comes to Earth because of precipitation over several months with a half-residence time of 30 days (Glasstone and Dolan 1977, p. 446). UNSCEAR (2002, Annex C, Fig. 5, p. 164) contains the nuclear deposition (Sr-90) data used in the analysis. More intense ground and tropospheric tests reach the stratosphere, which is relatively isolated from the lower atmosphere; it takes about a year for stratospheric material to settle into the troposphere (UNSCEAR 2002, p. 162). Nuclear bomb testing also occurred in the stratosphere (Glasstone and Dolan 1977, 446–448). Some nuclear tests, including the very

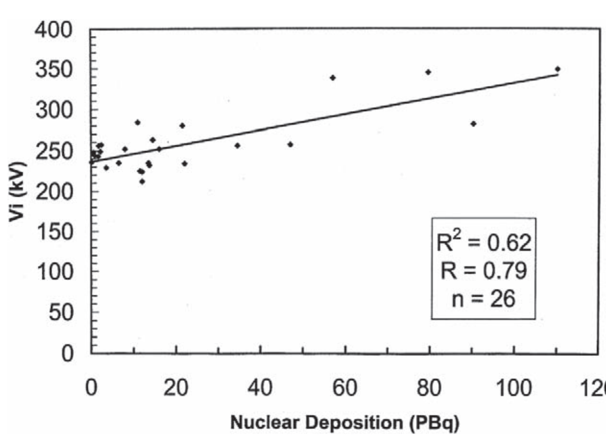

Fig. 5. Correlation of Vi with ground-level Sr-90 nuclear deposition using Vi data one year after the fallout data.

high-yield Starfish test in 1962, were conducted in the mesosphere where the radioactive debris would have settled into the stratosphere.

Nuclear material in the stratosphere rather than fallout on the ground is a better measure of the ionization in the upper troposphere that could influence conductivity above the global thunderstorm generator and its ability to maintain the global circuit. Thus, a second analysis was performed using the available Strontium-90 "stratospheric burden" data that end in 1974 (Glasstone and Dolan 1977, 448–450), allowing the correlation to be studied from 1954 through 1974. Figure 6 gives the correlation between stratospheric Sr-90 and Vi with a 1 yr lag: $R = 0.86$ ($p<0.001$). With no lag $R = 0.70$ and with a lag of 2 yr $R = 0.53$. The stratospheric radiation is more highly correlated with Vi than the ground-level radiation, again the maximum correlation is with a lag of 1 yr.

In studying the effect of nuclear testing on the global circuit and Earth's electric field, conditions at ground level should be considered. Here the enhanced ionization just above the ground from fallout causes conductivity to increase resulting in an inversely proportional decrease of electric field intensity as found in various parts of the world (Pierce 1972; Collingbourne 1972).

It is concluded that the enhancement of Vi by as much as 40% in the 1960–65 period was caused by nuclear radiation in the upper troposphere and lower stratosphere. By 1966 both atmospheric radiation and Vi dropped back to their baseline values prior to enhanced nuclear testing (Fig. 4). The mean of Vi computed for the period 1966 through 2004 is 240 kV. From a few years after the end of nuclear testing until the most recent measurements in 2004, Vi values have remained essentially constant within ±10% of the mean. This finding contradicts reports that over the last 39 years the global circuit intensity has decreased by 44% (Märcz and Harrison 2003).

COSMIC RADIATION AND THE GLOBAL CIRCUIT.

An early speculative article on sun–weather relationships proposed a mechanism in which increased ionization from cosmic radiation over the global cloud electrical generator reduced the resistance above the global generator causing an increase in the charging current to the global circuit (Markson 1978). Supporting evidence was both from the negative correlation between solar wind velocity and Vi (Markson and Muir 1980) and positive correlation between galactic cosmic radiation and Vi (Markson 1981); this is consistent because solar wind velocity is inversely correlated with cosmic radiation.

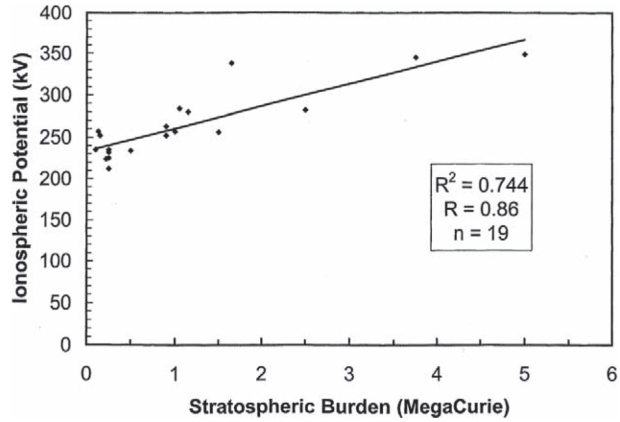

Fig. 6. Correlation of Vi with stratospheric Sr-90 using Vi data one year after the stratospheric burden data.

The conclusion was that cosmic ionizing radiation must increase Vi by affecting the generator part of the circuit because if the modulation were in the fair-weather return-path part of the circuit it would lower the global columnar resistance by essentially partially shorting out Vi, causing it to decrease. The present finding that atmospheric nuclear radiation, much of it residing in the stratosphere from months to a few years after the explosions, was positively correlated with Vi supports the cosmic radiation–Vi hypothesis. This is because the nuclear radiation would enhance ionization above, near, and within the convective clouds in the same way as cosmic radiation provides enhanced ionization in these regions.

ANNUAL VARIATION.

The annual variation of global geoelectric potential intensity is not known. Atmospheric electrical textbooks present figures from data obtained at ground level in the Northern Hemisphere showing a maximum of electric fields in the winter and minimum in the summer (Chalmers 1969, p. 169; Israël 1973, p. 351). But ground-based measurements of electric field and air–Earth current are so influenced by variations in local aerosol that globally representative values cannot be determined. In the winter, aerosol loading of the lower atmosphere maximizes for many reasons, including more burning of fuel, reduced atmospheric circulation and low inversions (Adlerman and Williams 1996). The aerosols also grow due to higher relative humidity (Pruppacher and Klett 1978), causing a decrease in conductivity resulting in electric field intensity in the lower atmosphere to be larger in winter than in summer.

The seasonal variation of temperature between ±60° latitude that would modulate the global circuit intensity shows a single cycle variation in surface temperature maximizing in August (Williams

1994). Since the vertical temperature gradient in the lower atmosphere increases with temperature near the ground and is the major factor controlling convective activity, and most of the world's landmass, where deep convection occurs, is in the Northern Hemisphere, thunderstorms and deep convection should maximize in the summer.

The annual monthly variation of Vi (Fig. 7) was determined using the complete diurnally normalized Vi data set (Table 1). To minimize sampling error, all measurements made on a single day or within three consecutive days were averaged into a single value. The figure gives the number of such values used for each month. The curve is relatively flat but there is an approximate 10% increase to a maximum in August with the curve remaining elevated in September and October and subsequently returns to its original quasi-stable value. From the available data it is not possible to identify a minimum month. The values for November through January are more variable and not as reliable because of the relatively small number of observations in these months. It appears that the winter months are lower than the rest of the year since November and January are low while the high value in December may be due to there being only six measurements that were obtained in 1955 and 1956, a period of increasing nuclear testing. The maximum occurs in August, the same month as the maximum of air temperature at mid and low latitudes (Williams 1994). The average of the monthly Vi averages is 242 kV.

For comparison, the air–Earth current at Kew in the United Kingdom has a periodic variation with a maximum in August and minimum in January as in this analysis (Chalmers 1967, p. 234). Air–Earth current is a better indicator of global circuit conditions than electric field intensity as it is controlled by the total Earth-to-ionosphere columnar resistance and thus is less sensitive to pollution and space charge variations that occur near the ground. The electric field intensity maximizes in the winter at Kew because pollution maximizes in the winter. A summary of many years' measurements from continental stations shows the maximum electric field occurs in the winter (Israël 1973, p. 353)—the same pollution effect as at Kew being present over land stations in both hemispheres. Ocean measurements by the Carnegie have also reported a maximum in the winter (Israël 1973, p. 353), but reanalysis of the Carnegie data in which non-fair-weather values were excluded shows the maximum was in July (Adlerman and Williams 1996).

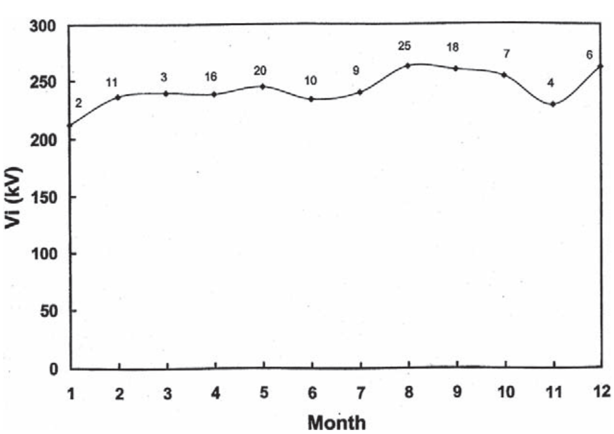

Fig. 7. Monthly variation of Vi. The number of points used to obtain the monthly averages are shown.

The only previous analysis of Vi data by month (Fischer 1962) shows a maximum in the winter. However, reviewing these records shows that during the three years of his measurements (1959–61) April through September had few measurements—11 on 9 days over 3 years (June and August had none)—so it is likely that sampling error led to the conclusion that Vi in the winter was larger than in the summer. In the analysis reported here (Fig. 7) the months April through September had 98 data points. There actually were many more measurements, but to make these data independent, measurements made within a 3-day period were averaged into a single number. If this procedure were used for the Fischer data, there would be only four points to represent the 6-month period.

IONOSPHERIC POTENTIAL COMPARED TO GLOBAL LIGHTNING ACTIVITY: DIURNAL AND SEASONAL VARIATIONS.

The global circuit discussed so far involves a DC flow of current through a closed loop driven by convective cloud electrification. However, some of these clouds (thunderclouds) also create an AC global circuit in which lightning causes global-scale electromagnetic signals. The Schumann resonances phenomenon detects lightning activity from all over the world with a single sensor (Schumann 1952; Clayton and Polk 1977; Sentman and Fraser 1991). This is possible because the conductive Earth surface and ionosphere constitute a spherical capacitor that has a resonant frequency in the ELF (extremely low frequency: 3–30 Hz) range where much of the energy in cloud-to-ground lightning resides—a single ground flash causes the cavity to resonate and a single receiver anywhere can detect the electromagnetic discontinuity. The nodal structure of resonant wave phenomena and changes in the ionosphere affect the signal strength relative to the receiver's position so several stations around the world are necessary to obtain globally representative data. The average diurnal variation of Schumann resonances is on the order of 50%–75% of its mean value (Heckman et al. 1998; Williams and Sátori 2004; Price and Melnikov 2004), about twice the 33% Carnegie curve diurnal variation. The annual variation is also on the order of 50%–75% of its mean value (Price and Melnikov 2004: Williams and Sátori 2004), about 3–4 times the 15% of mean estimate of Vi variation (Fig. 7).

These differences indicate that the global DC generator is supported mostly by the smaller currents from electrified shower clouds that cover relatively large areas and not, as generally believed, by the larger currents from thunderstorm clouds that cover only a relatively small fraction of Earth's surface (Wilson 1920; Imyanitov and Chubarina 1967; Williams and Heckman 1993). The relatively constant global-scale convective activity would produce flatter diurnal and annual variations of Vi than the variation of global thundercloud activity. The diurnal variation due to convection has three sharp peaks every day during the afternoon over the three major continental landmasses: Africa, the Americas, and the Maritime Continent in the western Pacific (see Fig. 1; Williams and Heckman 1993). The relatively flat seasonal variation of Vi with a maximum in late summer is explained if most of the electrified shower clouds are in the Tropics since the ratio of land-to-ocean area is relatively constant through the Tropics with about 26% in the Northern Hemisphere and 23% in the Southern Hemisphere (Williams 1994).

The temporal and spatial variation of global lightning also is observed with an optical sensor on satellites. NASA has been operating an Optical Transient Detector (OTD) since 1995 that samples all regions of the Earth making lightning about twice a day (Christian et al. 2003); these data show a globally averaged annual variation of 44%, similar to the Schumann resonances annual variation (Sátori et al. 1999). The peak month in the annual lightning variation observed from space is August, which is the month with maximum in the annual variation of Vi and highest surface air temperature within 60° of the equator.

TEMPERATURE MODULATION OF THE GLOBAL CIRCUIT.

The ability to measure global lightning variation and Vi makes it possible to study the effects of global temperature on convective cloud activity. The term global temperature is used in the sense of Hansen and Lebedeff (1987) in their seminal paper on "global warming" where they studied global surface air temperature with data from continental and island locations. One may question whether the temperature data in the Vi comparison study (to be discussed), which was for the latitude belt from 15°N to 30°S across Africa and the Americas, were globally representative since 71% of the world's surface is ocean. Hansen and Lebedeff (1987) have shown high correlation between temperatures at locations separated by as much as 1000 miles for all latitude belts and between the Northern and Southern Hemispheres. Since most of the ocean areas are in the Southern Hemisphere and temperatures from both hemispheres were correlated, the conclusion is that the land areas provide globally representative temperature data.

Schumann resonances have been found by Williams (1992) to be positively correlated with the tropical surface temperature anomaly described by Hansen and Lebedeff (1987); they also were correlated with Vi (Williams 1992). The Schumann resonances–global temperature relationship stimulated interest in the scientific community because Schumann resonances analysis provides a simple method with only a few land-based sensors to monitor global thunderstorm activity. Subsequent studies showed that a 1% change in global surface temperature was associated with a 15%–20% increase in Vi, presumably by stimulating convection (Markson and Lane-Smith 1994; Markson and Price 1999). The same sensitivity estimate was obtained using cloud-top heights as a measure of global thunderstorm activity (Price 1993).

To study the relationship of temperature to Vi, two investigations obtained high temporal resolution temperature data in equatorial and tropical Africa and South America—the latitudes containing the majority of global thunderstorms (Markson and Lane-Smith 1994; Markson 2003). This analysis utilized hourly "aviation routine weather report" (METAR) ground-level temperatures at airports to perform 1-h-resolution lag analysis between the time of the Vi sounding (a benchmark) and temperature before and after the sounding—this time resolution provided insight into mechanisms.

The first program compared temperature in the 20°N–20°S latitude band and Vi; analysis of 31 balloon soundings at Weston found significant positive correlations (Markson and Lane-Smith 1994). For Africa, the correlation maximized (R=0.6) when the temperature 5 hours before the sounding was used; for South America it maximized (R=0.8) when the temperature 2 h before the soundings was used. This is consistent because maximum heating

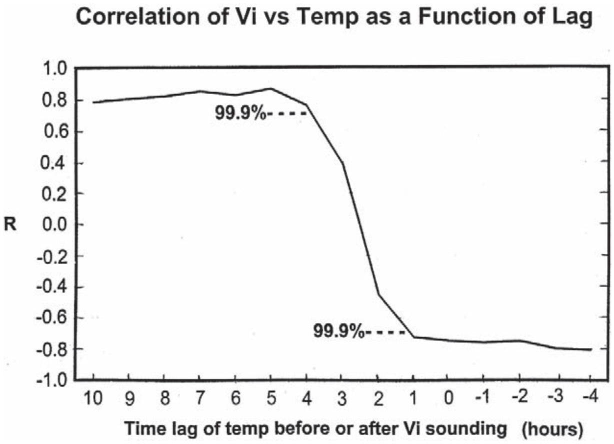

Fig. 8. The variation of correlation coefficient between Vi and temperature over Africa and South America as a function of lag from 10 h before until 4 h after the sounding. The *p*<0.001 probability levels are shown.

occurs about 3 h earlier UTC in Africa than in South America.

A subsequent experiment with more detailed analysis over a larger range of lags in March 1998 used 19 balloon soundings at Orlando, Florida (Markson 2003), and temperature from 15°N to 30°S. This work demonstrated not only that temperature controlled Vi variation but also that a negative feedback mechanism existed—warmer-than-average temperature in the morning led to an increase in Vi, presumably due to more deep convection and electrified clouds, but temperature rise in the afternoon was inhibited by increased cloud screening of radiation.

In Fig. 8 the lag analysis of correlation coefficient variation between Vi and the combined temperature for both continents from 15°N to 30°S is calculated with temperatures averaged over approximately equal size areas (15° × 15° boxes) in Africa and South America to remove biasing due to differences in the density of reporting stations. There is high positive correlation in the morning and high negative correlation in the midafternoon through evening presumably due to the clouds from the enhanced morning convection shielding afternoon solar radiation. This phenomenon is well recognized: morning and midday convective development leads to overdevelopment of clouds, reduced temperatures due to shading, and minimal thermal activity later (e.g., see Fig. 9).

Fig. 9. Thunderstorm clouds can shield large areas cutting off further heating and reducing subsequent convective activity.

The sensitivity of Vi to temperature is shown in Fig. 10. For temperatures 7 h before the sounding (lag 7), an 8°C increase in temperature corresponds to a 100-kV increase in Vi, that is, 1% increase in temperature is associated with a 16% increase in Earth's electric field intensity. Significant positive correlations persisted when the Vi measurements made during the afternoon in Africa and South America were analyzed separately using the same lags.

To investigate if cloud screening of radiation caused initially a positive and then negative correlation of Vi versus temperature, separate analyses were conducted for Africa and South America (Markson 2003; Fig. 11). For both continents, the higher the noon temperature, the smaller the difference between the noon and 1500 LT maximum temperature. In other words, if noon temperatures typically are 2°C cooler than the maximum daily 1500 LT temperatures, warmer-than-average noon temperatures might be only 1°C cooler than 1500 LT temperatures because cloud screening reduced the rise of afternoon temperature.

These mechanisms—where a warm morning creates convection and residual clouds inhibiting radiational heating later in the day—indicate a negative feedback process that on the diurnal time scale would tend to stabilize temperature. However, on a longer global warming time scale, positive feedback should occur because increased thunderstorm

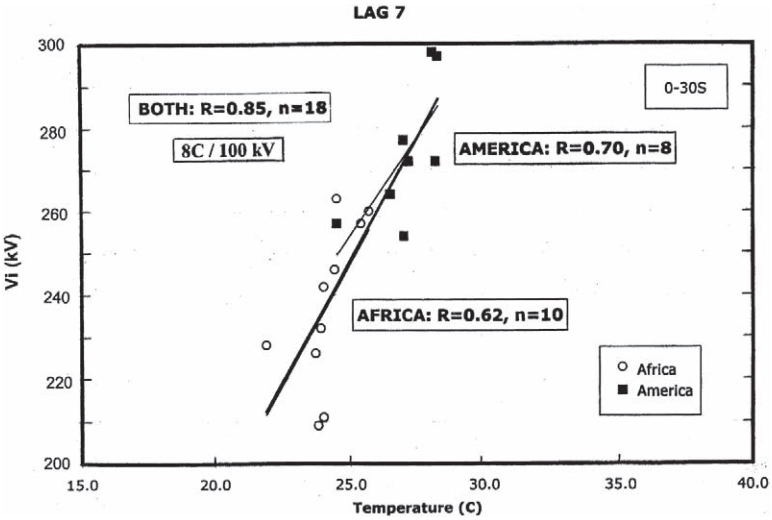

Fig. 10. Correlation of the variation of temperature with Vi for lag 7 h (temperature earlier than the sounding). The slopes of the lines of regression for Africa, America, and both continents combined are similar and indicate that a 1% change in temperature leads to a 16% increase in Vi. (Note: The line of regression for the African soundings is almost coincident with the one for the combined data.)

activity would pump more water vapor into the atmosphere.

DEEP CONVECTIVE CLOUDS AND GLOBAL WARMING. In global warming discussions it rarely is mentioned that most of the reported signal comes from increases in nighttime temperature (Karl et al. 1993; Easterling et al. 2000). This could be caused by the residue clouds from daytime thunderstorms and deep convection, which produce large areas of cirrus and other residue clouds and water vapor that remain in the night sky. Nighttime radiational cooling of Earth's surface is inhibited by cloudiness, and water vapor is the dominant greenhouse gas. Deep convection is particularly important because a water vapor molecule at 12 km is 1000 times as effective as a greenhouse gas as one near the surface (Lindzen 1997). It has been found that ELF/Schumann resonances radiation produced by lightning is highly correlated with water vapor in the upper troposphere, which is transported there by thunderstorms (Price 2000; Price and Asfur 2006). Thus, increased convective activity should increase nighttime temperature in particular and contribute to the global warming signal.

CONCLUSIONS. Study of ionospheric potential variation can enhance understanding of Earth's electric field and how it can be modulated by natural and anthropogenic processes. The following is a summary of the findings and relevance of the global circuit and related phenomena to global change research:

1) Atmospheric nuclear testing was highly correlated with an increase in global circuit intensity by as

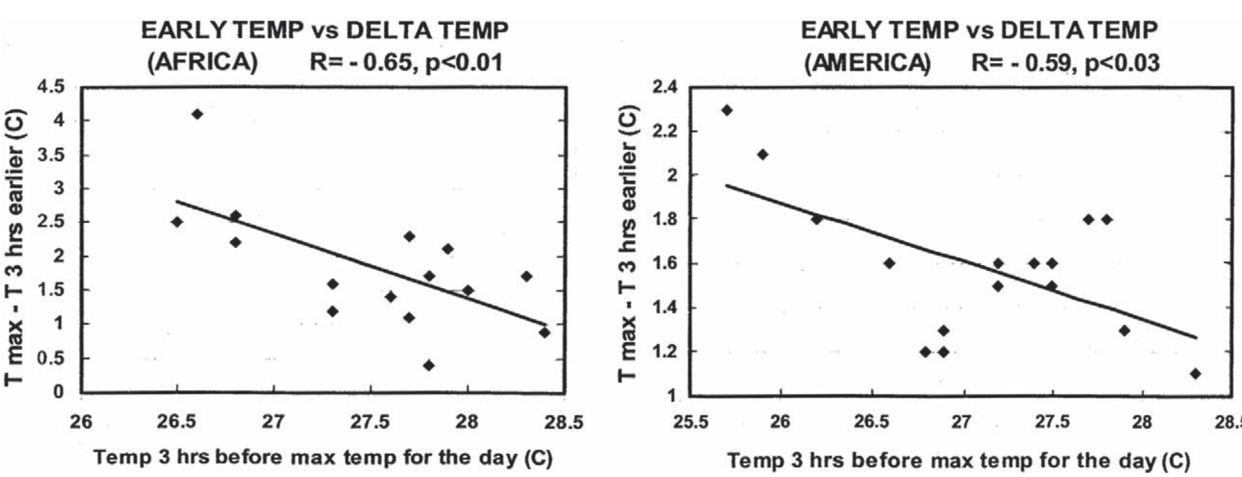

Fig. 11. Correlation of the difference between maximum afternoon temperature (3 pm) and noon temperature compared to noon temperature for (a) Africa and (b) South America. These analyses indicate the warmer the noontime temperature the less the increase in temperature until midafternoon. This suggests that increased thermally driven convection increases cloud screening of incoming longwave radiation.

much as 40% during the period 1960 through 1964.

2) Following the nuclear test period there has been no apparent secular variation in Vi, which has averaged 240 kV, since 1966. This indicates that recent reports of the Earth's electric field intensity decreasing during the twentieth century are not valid.
3) The positive correlation between atmospheric nuclear radiation and Vi supports the hypothesis that galactic cosmic radiation modulates the intensity of the global circuit through changes in ionization over and near deep convective clouds.
4) The annual maximum to minimum variation of Vi is on the order of 15% of the mean with an apparent maximum in August. This month also is the maximum period in the annual variation of lightning observed from space and global surface air temperature in the ±60° latitude zone. The minimum of Vi occurs in the Northern Hemisphere winter season but the specific month can not be identified.
5) Temperature over Africa and South America are positively correlated with Vi in the morning and negatively correlated with Vi in the afternoon. The apparent reason is that enhanced morning convective activity leads to greater afternoon cloudiness that shields the ground from solar radiation later in the day.
6) Ionospheric potential measurement is a means of monitoring global thunderstorm and electrified convective shower cloud activity. This convection provides all the upward transport of water vapor to the upper troposphere and stratosphere, and water vapor is the most important greenhouse gas contributing to global warming both day and night. Thus temperature-enhanced deep convection provides positive feedback to global warming.
7) Nocturnal clouds and water vapor from the previous day's convective activity will reduce the rate of radiational cooling at night. This may explain why most of the observed global warming signal comes from higher nighttime temperatures.
8) It is not possible to compare the long-term variation of Vi to global warming since the sensitivity ratio of Vi to temperature by percent is 16% to 1%. Thus the reported approximate 0.4°C increase in global temperature over the last four decades (Jones et al. 2001), a 0.1% change in temperature, would produce too small an effect (1.6% = 4 kV) to be detected in the past Vi data. In the future, with further refinement of measurements, Vi variation may provide a relatively simple method to study global change.

Study of the global circuit variation is attractive in global change research because a globally representative parameter modulated by temperature can be observed with a single measurement. Past global temperature variation data have utilized hundreds of ground-level measurements in all parts of the world and complex satellite technology. Measurement of the global circuit offers new methodology for study of worldwide meteorological processes and provides additional insight into mechanisms influencing climate change. While attention to the global warming problem has focused on anthropogenic activity and CO_2 emission, natural convective activity, which can be monitored through variation of the DC and AC global circuits, must play a central role in climate change.

ACKNOWLEDGMENTS. Support for the global circuit research and Vi measurements over the years at MIT and Airborne Research Associates came from several sources: ONR (N00014-71-C-0156 and N00014-74-C-0336), NSF (ATM-8211403, Award 9016942 and 9160660, Grant DMI-9304487), and NASA (NRG22-009-727, NAS6-3203, NAS8-84771). I thank Dan Vogel, Carnegie Mellon University, for help with the Orlando Vi soundings and data analysis. Richard Ferris, Manager, MIT Lincoln Lab, Orlando Field Site, provided the facilities for the Orlando Vi measurements. The Australian Meteorological Service in Darwin, Jim Arthur, Head, was particularly helpful in supporting the Vi measurements in Darwin. Thanks to Gabriella Sátori, Colin Price, and Giles Harrison for providing data and information during preparation of this article. Useful comments were offered by Chris Fairall and Lothar Ruhnke. Review comments by Earle Williams and Dave Sentman were particularly valuable. The picture of thunderstorm clouds shading the ground (Fig. 9) was provided by Walt Lyons.

APPENDIX: DESCRIPTION OF AIRCRAFT, FLIGHT PROCEDURES, AND INSTRUMENTATION USED TO OBTAIN IONOSPHERIC POTENTIAL MEASUREMENTS. Figure A1 is a picture of the Beechcraft TurboBaron Model 56 TC used to obtain ionospheric potential soundings since 1980. Turbocharged 380 hp engines provide a ceiling of 10 km. It is flown at 5 m above the ocean at the start of up soundings and at the end of down soundings. The aircraft soundings are always made over the ocean in the same local region (columnar resistance volume) that is free of clouds. The vertical electric field is determined from the potential difference between radioactive ionizing probes located 1/2 m above and below the wingtip; the potential difference between the probes divided by the distance between them is the electric field. The ionizing units bring the electrodes to the atmospheric potential at their height. High-impedance electrometers and associated electronics are located in the wingtip to reduce capacitance of the input, which minimizes response time to less than 1 s.

FIG. A1. Beechcraft TurboBaron aircraft used for measurements of ionospheric potential. The vertical fair-weather electric field is measured between the radioactive probes above and below the wingtip. The picture was taken at Andros Island, Bahamas, a region where many of the past ionospheric potential soundings have been obtained over nearby ocean areas.

Most electric field measuring systems use a high-ohm carbon film resistance ($10^{12}\Omega$) at the input so as not to load the input resistance of the ion cloud. But such an arrangement requires extremely good insulation, which is hard to maintain in a marine environment and carbon film resistors are unstable and change their value with temperature and voltage. The Baron system uses a negative feedback circuit to eliminate the need for a high-ohm resistor and maintenance of extreme insulation for the electrodes. In this system a high-voltage power supply drives a guard ring around the electrodes to the potential of the electrodes and the power supply voltage is measured to obtain the electrode potential. The guard ring being at the same potential as the electrode eliminates leakage current from the electrode to ground. The power supply can keep the guard ring at the electrode potential despite any small leakage current from the guard ring to ground.

Obtaining reliable electric field measurements from aircraft is difficult because the charge on the aircraft, mostly due to the engine exhaust, creates an electric field that is superimposed on the ambient field to be measured. To overcome this problem the aircraft electric field is common-mode rejected by locating the top and bottom electrodes in the same equipotential surface around the wingtip arising from aircraft charge. Thus, the same potential due to aircraft charge is applied to both probes but the fields due to aircraft charge are in opposite directions above and below the wing. Therefore, the field above the wing due to aircraft charge adds to the potential of the top probe the same amount as the field below the wing reduces the potential of the bottom probe and the potential difference between the probes in this balanced condition remains the same regardless of aircraft charge.

The entire aircraft system is calibrated through a series of low passes by a ground station. Calibration cannot be done in the Earth's surface because the aircraft would be at ground potential and mirror image effects in the conducting ground.

REFERENCES

Adlerman, E. J., and E. Williams, 1996: Seasonal variation of the global electrical circuit. *J. Geophys. Res.,* **101,** 29 679–29 688.

Ault, J. O., and S. J. Mauchly, 1926: Ocean magnetic and electric observations obtained aboard the Carnegie, 1915–21. *Pub. Carnegie Inst.,* **175,** 197–286.

Bering, E. A., III, A. A. Few, and J. R. Benbrook, 1998: The global electric circuit. *Phys. Today,* **51,** 24–30.

Bhartendu, 1971: Correlations of electric potential gradients at land stations and their implication on the classical picture of atmospheric electricity. *Pure Appl. Geophys.,* **84,** 13–26.

Blanchard, D. C., 1963: Electrification of the atmosphere by particles from bubbles in the sea. *Progress in Oceanography,* Vol. 1, McMillan, 71–202.

Burns, G. B., A. V. Frank-Kamenetsky, O. A. Troshichev, E. A. Bering, and B. D. Reddell, 2005: Interannual consistency of bi-monthly differences in diurnal variations of the ground-level, vertical electric field. *J. Geophys. Res.,* **110,** D10106, doi:10.1029/2004JD005469.

Chalmers, J. A., 1967: *Atmospheric Electricity.* 2d ed. Pergamon, 515 pp.

Christian, H. J., and Coauthors, 2003: Global frequency and distribution of lightning as observed from space by the Optical Transient Detector. *J. Geophys. Res.,* **108** (D1), 4005, doi:10.1029/2002JD002347.

Clark, J. F., 1956: The fair-weather atmospheric electrical potential and its gradient. Ph.D. thesis, University of Maryland, 151 pp.

——, 1958: The fair-weather atmospheric electrical potential and its gradient. *Recent Advances in Atmospheric Electricity,* Pergamon, 61–73.

Clayton, M., and C. Polk, 1977: Diurnal variation and absolute intensity of world-wide lightning activity, September 1970 to May 1971. *Electrical Processes in Atmospheres,* Steinkopff, 440–449.

Cobb, W. E., 1968: The atmospheric electric climate at Mauna Loa Observatory, Hawaii. *J. Atmos. Sci.,* **25,** 470–480.

Collingbourne, R. H., 1972: Comment on paper by E. T. Pierce, "Radioactive fallout and secular effects in atmospheric electricity." *J. Geophys. Res.,* **77,** 6634–6638.

Dolezalek, H., 1971: Introductory remarks on the classical picture of atmospheric electricity. *Pure Appl. Geophys.,* **84,** 9–12.

Easterling, D. R., T. R. Karl, K. P. Gallo, D. A. Robinson, K. E. Trenberth, and A. Dai, 2000: Observed climate variability and change of relevance to the biosphere. *J. Geophys. Res.,* **105,** 20 101–20 114.

Fischer, H. J., 1962: Die elektrische spannung zwischen ionosphäre und Erde. Ph.D. thesis, Technischen Hochschule Stuttgart, 124 pp.

Glasstone, S., and P. J. Dolan, 1977: *The Effects of Nuclear Weapons.* 3d ed. U.S. Department of Defense, U.S. Government Printing Office, 653 pp.

Hansen, J., and S. Lebedeff, 1987: Global trends in measured surface air temperature. *J. Geophys. Res.,* **92,** 13 345–13 372.

Harrison, G., 2002: Twentieth century secular decrease in the atmospheric potential gradient. *Geophys. Res. Lett.,* **29,** 1660, doi:10.1029/2002GL014878.

Heckman, S. J., E. Williams, and B. Boldi, 1998: Total global lightning inferred from Schumann resonances measurements. *J. Geophys. Res.,* **103,** 31 775–31 779.

Imyanitov, I. M., and E. V. Chubarina, 1967: *Electricity of the Free Atmosphere.* National Science Foundation, Washington, D.C., Israel Program for Scientific Translations, Clearinghouse for Federal Scientific and Technical Information, 212 pp.

Israël, H., 1973: Atmospheric Electricity. Vol. 2, National Science Foundation, Israel Program for Scientific Translations, National Technical Information Services, 338 pp.

Jones, P. D., T. J. Osborn, and K. R. Briffa, 2001: The evolution of climate over the last millennium. *Science,* **92,** 662–667.

Karl, T. R., and Coauthors, 1993: Asymmetric trends of daily maximum and minimum temperature. *Bull. Amer. Meteor. Soc.,* **74,** 1007–1023.

Kasemir, H., 1972: Atmospheric electric measurements in the Arctic and Antarctic. *Pure Appl. Geophys.,* **100,** 70–80.

Kraan, C., 1971: *Belgian Netherlands Antarctic Expedition 1966, Atmospheric Electricity.* Belgium, 134 pp.

Lindzen, R. S., 1997: Statement concerning global warming, U.S. Senate Committee on Environment and Public Works, 10 June 1987. [Available online at www.data-yard.net/historic/files/lindzen.htm.]

Lord Kelvin, 1860: Atmospheric electricity. Royal Institution Lecture, Papers on Electrostatics and Magnetism, 208–226.

Märcz, F., and R. G. Harrison, 2003: Long-term changes in atmospheric electrical parameters observed at Nagycenk (Hungary) and the UK observations at Eskdalemuir and Kew. *Ann. Geophys.,* **21,** 2193–2200.

Markson, R., 1975, Atmospheric electrical detection of organized convection. *Science,* **188,** 1171–1177.

——, 1976: Ionospheric potential variations obtained from aircraft measurements of potential gradient. *J. Geophys. Res.,* **81,** 1980–1990.

——, 1978: Solar modulation of atmospheric electrification and possible implications for the sun–weather relationship. *Nature,* **273,** 103–109.

——, 1981: Modulation of the Earth's electric field by cosmic radiation. *Nature,* **291,** 304–308.

——, 1985: Aircraft measurements of the atmospheric electrical global circuit during the period 1971–1984. *J. Geophys. Res.,* **90,** 5967–5977.

——, 1986: Tropical convection, ionospheric potentials and global circuit variation. *Nature,* **320,** 588–594.

——, 2003: Ionospheric potential variation from temperature change over continents. *Proc. 12th Int. Conf. on Atmospheric Electricity,* Versailles, France, Int. Committee on Atmos. Electricity, 283–286.

——, and M. Muir, 1980: Solar wind control of the Earth's electric field. *Science,* **208,** 979–990.

——, and D. Kendra, 1992: Ionospheric potential measurements at Hawaii and Christmas Island. *Proc. Ninth Int. Conf. on Atmospheric Electricity,*

St. Petersburg, Russia, Int. Committee on Atmos. Electricity, 18.
——, and D. Lane-Smith, 1994: Global change monitoring through the temporal variation of ionospheric potential. Preprints, *Fifth Symp. on Global Change Studies,* Nashville, TN, Amer. Meteor. Soc., 279–287.
——, and C. Price, 1999: Ionospheric potential as a proxy index for global temperature. *Atmos. Res.,* **51,** 309–314.
——, L. H. Ruhnke, and E. R. Williams, 1999: Global scale comparison of simultaneous ionospheric potential measurements. *Atmos. Res.,* **51,** 315–321.
Mühleisen, R., 1971: New determination of the air–Earth current over the ocean and measurements of ionosphere potentials. *Pure Appl. Geophys.,* **84,** 112–115.
Novakov, T., V. Ramanathan, J. E. Hansen, T. W. Kirchstetter, M. Sato, J. E. Sinton, and J. A. Sathaye, 2003: Large historical changes of fossil-fuel black carbon aerosols. *Geophys. Res. Lett.,* **30,** 1324, doi:10.1029/2002GL016345.
Pierce, E. T., 1972: Radioactive fallout and secular effects in atmospheric electricity. *J. Geophys. Res.,* **77,** 482–487.
Pomelov, V., cited 2003: Water sampling of the subglacial Lake Vostok. Institute of Geoecology, Arctic and Antarctic Research Institute, Russian Antarctic Expedition, section 3.3. [Available online at http://south.aari.nw.ru/docs/water_sampling_lake_vostok.pdf.]
Price, C., 1993: Global surface temperatures and the atmospheric electrical circuit. *Geophys. Lett.,* **20,** 1363–1366.
——, 2000: Evidence for a link between global lightning activity and upper tropospheric water vapor. *Nature,* **406,** 290–293.
——, and A. Melnikov, 2004: Diurnal, seasonal and inter-annual variations in the Schumann resonances parameters. *J. Atmos. Solar-Terr. Phys.* **66,** 1179–1185.
——, and M. Asfur, 2006: Can lightning observations be used as an indicator of upper-tropospheric water vapor variability? *Bull. Amer. Meteor. Soc.,* **87,** 291–298.
Pruppacher, H. R., and J. D. Klett, 1978: *Microphysics of Clouds and Precipitation.* Reidel, 83 pp.
Richmond, A. D., 1986: Upper-atmosphere electric field sources. *Studies in Geophysics, The Earth's Electrical Environment,* National Academy Press, 224–227.
Roble, R., and I. Tzur, 1986: The global atmospheric electrical circuit. *Studies in Geophysics, The Earth's Electrical Environment,* National Academy Press, 224–227.
Sátori, G., E. R. Williams, B. Zieger, R. Boldi, S. Heckman, and K. Rothkin, 1999: Comparison of long-term Schumann resonances records in Europe and North America. *Proc. 11th Int. Conf. on Atmospheric Electricity,* Guntersville, AL, NASA/CP-1999-209261, 705–708.
Schumann, W. O., 1952: Propagation of very long electric waves and of lightning discharge around the Earth (translated). *Z. Naturforsch. Teil A,* **7,** 149–154.
Sentman, D. D., and B. J. Fraser, 1991: Simultaneous observations of Schumann resonances in California and Australia. *J. Geophys. Res.,* **96,** 15 973–15 984.
Torreson, O. W., O. H. Gish, W. C. Parkinson, and G. R. Wait, 1946: Scientific results of cruise VII of the Carnegie during 1928–29. Carnegie Institute Tech. Rep. 568, 176 pp.
UNSCEAR, 2002: Sources and effects of ionizing radiation. U.N. Scientific Committee on the Effects of Atomic Radiation (UNSCEAR), Vol. 1, Annex C, 158–167.
Whipple, F. J. W., and F. J. Scrase, 1936: Point discharge in the electric field of the Earth. *Geophys. Mem., London,* **68,** 1–20.
Williams, E. R., 1992: The Schumann resonances: A global tropical thermometer. *Science,* **256,** 1184–1187.
——, 1994: Global circuit response to seasonal variations in global surface air temperature. *Mon. Wea. Rev.,* **122,** 1917–1929.
——, 2003: Comment to "Twentieth century secular decrease in the atmospheric potential gradient" by Giles Harrison. *Geophys. Res. Lett.,* **30,** 1803, doi:10.1029/2003Gl017094.
——, and S. Heckman, 1993: The local diurnal variation of cloud electrification and the global diurnal variation of negative charge on the Earth. *J. Geophys. Res.,* **98,** 5221–5234.
——, and G. Sátori, 2004: Lightning, thermodynamic and hydrological comparison of the two tropical continental chimneys. *J. Atmos. Solar-Terr. Phys.,* **66,** 1213–1231.
——, R. Markson, and S. Heckman, 2005: Shielding effects of trees on the measurement of the Earth's electric field: Implications for secular variations of the global electrical circuit. *Geophys. Res. Lett.,* **32,** L19810, doi:10.1029/2005GL023717.
Wilson, C. T. R., 1920: Investigations on lightning discharges and on the electric field of thunderstorms. *Phil. Trans. Roy. Soc. London Ser. A,* **221,** 73–115.